3D high order seismic imaging salt domes in the context of RTM algorithm using adjoint-based methods.

Javier Abreu, Roland Martin, Jose Darrozes

May 2020

Content

1. General context
2. Methodology
3. Preliminar results.
4. Perspectives.

Salt dome basins in Mexico.

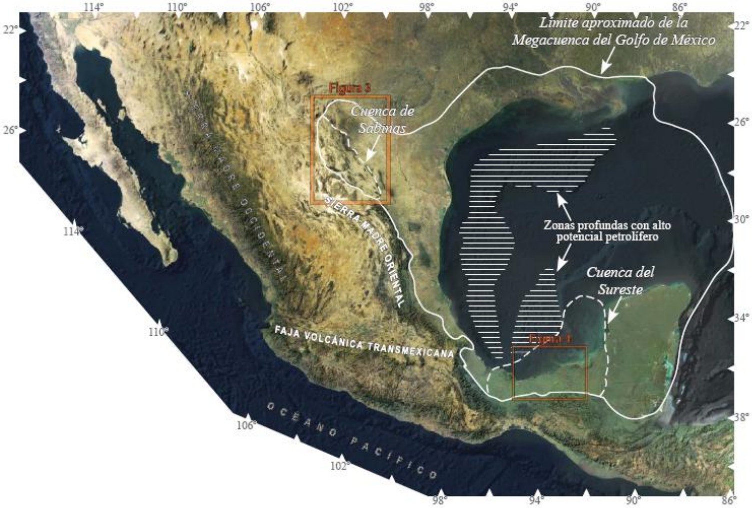

Figure 1: Mexican salt basin [García, 1983]

Characteristics of salt structures.

- High impermeability
- Change shape and flow through adjacent rocks.
- Generally they form a trap for oil and natural gas. Many hydrocarbon reservoirs are located in a context of salt tectonics.

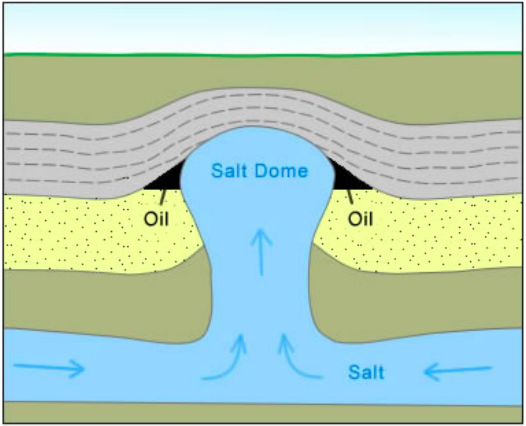

Characteristics of seismic images from salt domes.

- Bad quality below the salt structure.
- The base of the salt is not well defined.
- High concentration of noise attributed to multiples.

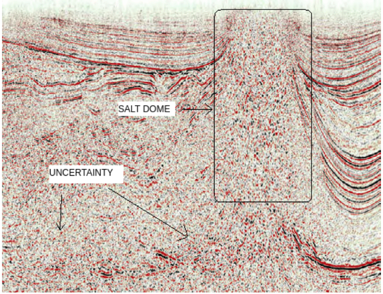

Figure 3: Example of a seismic image of a complex geology region including salt domes. Taken from [Buehnemann et al., 2002]

Seismic imaging.

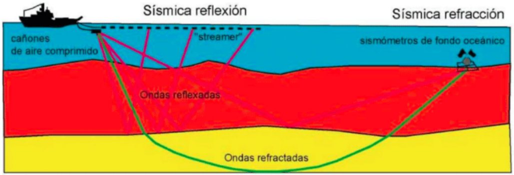

Figure 4: Forward model. Seismic data acquisition

$$\mathbf{d} = g(\mathbf{m}), \tag{1}$$

where g is an operator that relates the data $\mathbf{d}$ recorded by the receivers and the parameters from the subsoil $\mathbf{m}$.

Inversion techniques:

- Migration approach.
- Direct inversion.
- Inverse problem theory.

Elastodynamic equations.

We have to solve the elastodynamic equations, that govern the wave propagation through the subsoil. For lack of space, I show the 2D elastodynamic equations .

$$
\begin{aligned}
\rho\frac{\partial v_x}{\partial t} &= \frac{\partial \tau_{xx}}{\partial x} + \frac{\partial \tau_{xz}}{\partial z} + f_x,\\
\rho\frac{\partial v_z}{\partial t} &= \frac{\partial \tau_{xz}}{\partial x} + \frac{\partial \tau_{zz}}{\partial z} + f_z,\\
\frac{\partial \tau_{xx}}{\partial t} &= (\lambda + 2\mu)\frac{\partial v_x}{\partial x} + \lambda\frac{\partial v_z}{\partial z},\\
\frac{\partial \tau_{zz}}{\partial t} &= (\lambda + 2\mu)\frac{\partial v_z}{\partial z} + \lambda\frac{\partial v_x}{\partial x},\\
\frac{\partial \tau_{xz}}{\partial t} &= \mu(\frac{\partial v_x}{\partial z} + \frac{\partial v_z}{\partial x}).
\end{aligned}
$$

* $f_{x,z}$ could be point sources or moment tensors.

* Finite differences: Second order, staggered grids [Virieux, 1986].

* Absorbing boundary conditions (PML) [Komatitsch and Martin, 2007].

Reverse Time Migration based on adjoint theory.

Reverse Time Migration $\Rightarrow$ **RTM**

According to [Chang and McMechan, 1986], there are three stages in the algorithm:

- Forward modeling: Solution of the elastodynamic equation, we used point sources.
- Adjoint modelling: Solution of the elastodynamic equations in reverse time.
  *Adjoint source inversion:
  $f^{\dagger}(\boldsymbol{x}, t) = \sum_{r=1}^{nr} \left(\mathbf{u}(\boldsymbol{x_r}, T - t) - \boldsymbol{d}(\boldsymbol{x_r}, T - t) \right)$
  *Adjoint source migration: $f^{\dagger}(\boldsymbol{x}, t) = \sum_{r=1}^{nr} \boldsymbol{d}(\boldsymbol{x_r}, T - t)$
- Classical imaging condition
  *$I(\boldsymbol{x}) = \sum_{n=1}^{N} \boldsymbol{u}(\boldsymbol{x}, N + 1 - n)\boldsymbol{u}^{\dagger}(\boldsymbol{x}, n)$
  *Normalized by the forward wavefield: $I(\boldsymbol{x}) = \frac{\sum_{n=1}^{N} \boldsymbol{u}(\boldsymbol{x},N+1-n)\boldsymbol{u}^{\dagger}(\boldsymbol{x},n)}{\sum_{n=1}^{N} \left(\boldsymbol{u}(\boldsymbol{x},N+1-n\right)^2}$
  * Normalized by the adjoint wavefield: $I(\boldsymbol{x}) = \frac{\sum_{n=1}^{N} \boldsymbol{u}(\boldsymbol{x},N+1-n)\boldsymbol{u}^{\dagger}(\boldsymbol{x},n)}{\sum_{n=1}^{N} \left(\boldsymbol{u}^{\dagger}(\boldsymbol{x},N+1-n\right)^2}$

Sensitivity Kernels.

Misfit function $\Rightarrow \chi(\mathbf{m}) = \frac{1}{2}\sum_{r=1}^{nr}\int_0^T ||\boldsymbol{u}(\boldsymbol{x_r}, t, \mathbf{m}) - \boldsymbol{d}(\boldsymbol{x_r}, t)||^2 dt$.
Fréchet derivatives [Tromp et al., 2005], [Monteiller et al., 2015]:

$$\delta\chi = \sum_{r=1}^{nr}\int_0^T \left(\boldsymbol{u}(\boldsymbol{x_r}, t, \mathbf{m}) - \boldsymbol{d}(\boldsymbol{x_r}, t)\right) \cdot \delta\boldsymbol{u}(\overline{x_r}, t, \mathbf{m})dt$$

Fréchet derivatives with respect to the logarithm of velocity, density and Lamé coeficients.

$$\begin{aligned}
K_\rho(\boldsymbol{x}) &= -\int_0^T \rho(\boldsymbol{x})u^\dagger(\boldsymbol{x}, T-t)\cdot\partial_t^2 u(\boldsymbol{x}, t)dt, \\
K_\kappa(\boldsymbol{x}) &= -\int_0^T (\lambda(\boldsymbol{x}) + 2\mu(\boldsymbol{x}))\nabla\cdot u^\dagger(\boldsymbol{x}, T-t)\nabla\cdot u(\boldsymbol{x}, t)dt, \\
K_\mu(\boldsymbol{x}) &= -2\int_0^T \mu(\boldsymbol{x})\nabla u^\dagger(\boldsymbol{x}, T-t) : \nabla u(\boldsymbol{x}, t)dt, \\
K_\beta(\boldsymbol{x}) &= 2(K_\mu - \frac{4}{3}\frac{\mu}{\kappa}K_\kappa), \quad K_\alpha(\boldsymbol{x}) = 2(\frac{\kappa + \frac{4}{3}\mu}{\kappa})K_\kappa.
\end{aligned}$$

Parameters and characteristics of the code to solve the 3D simulation.

We use UniSolver to solve the elastodynamic equation showed previously, which is a FORTRAN, high order, finite differences-based code in 3 dimension and following a parallel approach. We use supercomputers and we also applied boundary conditions of the CPML type [Komatitsch and Martin, 2007], [Martin et al., 2010]. We use point sources.

Receptors $\Rightarrow$ 500.
Sources $\Rightarrow$ 250.
Frequency $\Rightarrow$ 4[Hz]
Longitude x$\Rightarrow$ 400(m)
Longitude y$\Rightarrow$ 3600[m]
Longitude z$\Rightarrow$ 9680.0[m]
Total time $\Rightarrow$ 3.825(s)
$\Delta x \Rightarrow 8.0[m], \ \Delta y \Rightarrow 8.0[m], \ \Delta z \Rightarrow 8.0[m], \ \Delta t \Rightarrow 0.00045[s]$
nx$\Rightarrow$ 50, ny$\Rightarrow$ 450, nz$\Rightarrow$ 1210, nt$\Rightarrow$ 8500

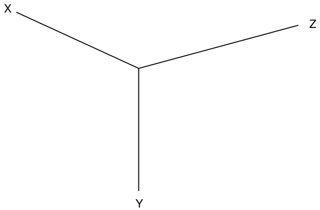

Velocity and density salt dome models.

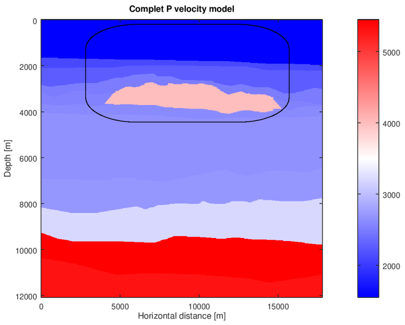

Figure 5: P velocity model $[m/s]$

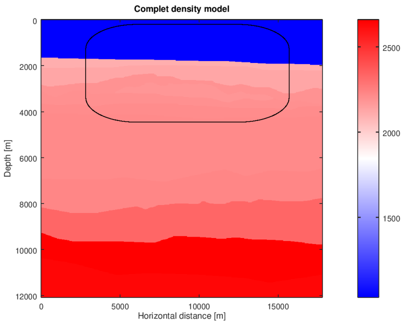

Figure 6: Density model $[kg/m^3]$.

Example of a 2D forward propagation.

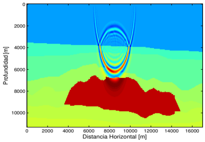

(a) $t = 1.525s$.

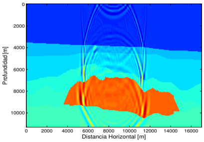

(b) $t = 2.275s$.

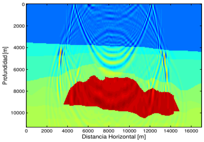

(c) $t = 3.275s$.

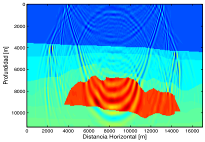

(d) $t = 3.775s$.

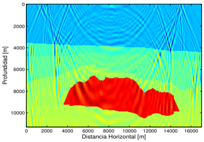

(e) $t = 4.775s$.

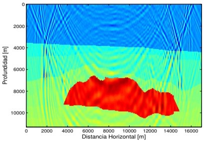

(f) $t = 5.275s$.

Figure 7: Snapshots from the forward propagation.

Principal methods used to attenuate multiples.

- SRME methods [Verschuur and Berkhout, 1992], which use the predictability feature of surface related multiples to predict and attenuate them.
- Change of domain methods, sometimes the multiples can be separated from the data in another domain, the most common one is the τ - p domain, (time of intercept and slowness).
- There are some approaches which use multiples as extra information and they do not attenuate them [Liu et al., 2015].

2D Kernels using simultaneous sources.

- We used a method based on CPML boundary conditions to attenuate the multiples.
- SB, TS, BS, S, and B represent the Sea bottom, top of the salt, base of the salt, sandstone and basement interfaces respectively.
- The kernel with multiple attenuation shows better definition in interfaces below the salt structure.

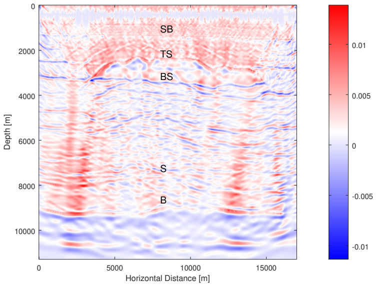

(a) Kernel lambda

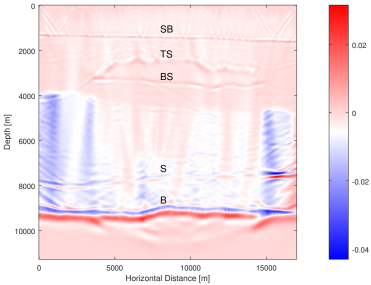

(b) Kernel lambda attenuation multiples

A priori model.

We assumed that we can know the bathymetry, below it we used a gradient with the maximal and minimal value of the real model.

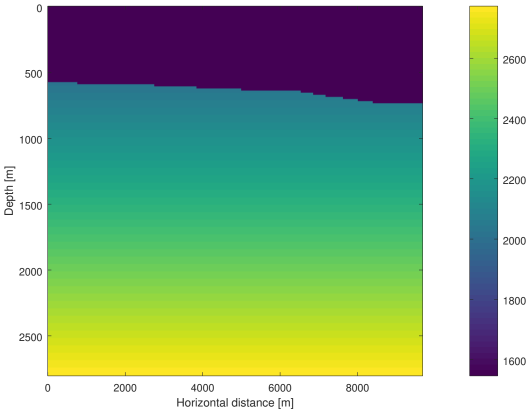

Figure 8: P velocity a priori model.

3D seismic sections with simultaneous sources.

The 3D simulations give more information of the model because they have a higher azimuth.

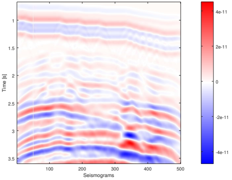

(a) Horizontal x component.

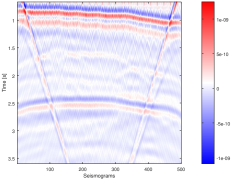

(b) Horizontal y component.

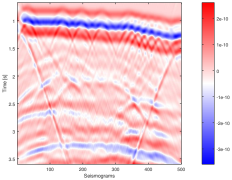

(c) Vertical component.

P velocity kernel simultaneous sources 3D.

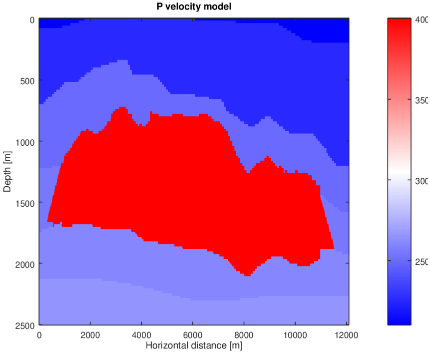

Figure 9: P velocity model.

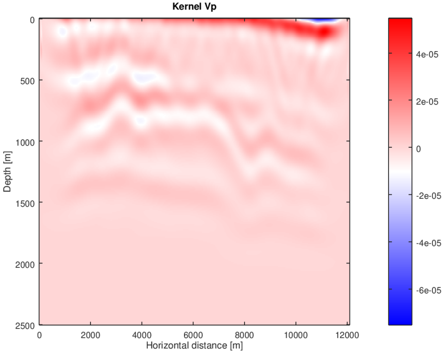

Figure 10: P velocity kernel

P velocity kernel separated sources 3D.

With separated sources the salt dome interfaces are reproduced almost as in the original model.

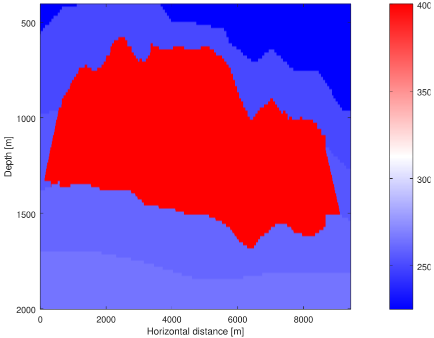

Figure 11: P velocity model.

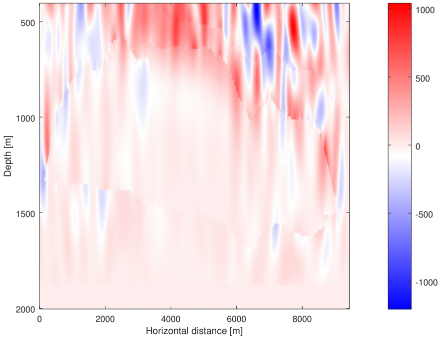

Figure 12: P velocity kernel obtained with separated sources.

Perspectives.

- Continue the development of the Full Waveform Inversion (FWI) in the UniSolver code in the context of an OBC simulation in order of attenuate the multiples in a more efective way.
- Application of the FWI to synthetic data related to complex geology (salt domes) together with gravity inversion.
- Application of the FWI in real hydro-geophysic data.

References I

Buehnemann, J., Henke, C. H., Mueller, C., Krieger, M. H., Zerilli, A., and Strack, K. M. (2002).
Bringing complex salt structures into focus—a novel integrated approach.
In *SEG Technical Program Expanded Abstracts 2002*, pages 446–449. Society of Exploration Geophysicists.

Chang, W.-F. and McMechan, G. A. (1986).
Reverse-time migration of offset vertical seismic profiling data using the excitation-time imaging condition.
Geophysics, 51(1):67–84.

García, L. B. (1983).
Domos salinos del sureste de mexico. origen: Exploracion: Importancia economica. in spanish. salt domes of southeastern mexico. origin: Exploration. economic importance.

References II

Komatitsch, D. and Martin, R. (2007).
An unsplit convolutional perfectly matched layer improved at grazing incidence for the seismic wave equation.
Geophysics, 72(5):SM155–SM167.

Liu, Y., Hu, H., Xie, X.-B., Zheng, Y., and Li, P. (2015).
Reverse time migration of internal multiples for subsalt imaging.
Geophysics, 80(5):S175–S185.

Martin, R., Komatitsch, D., Gedney, S. D., Bruthiaux, É., et al. (2010).
A high-order time and space formulation of the unsplit perfectly matched layer for the seismic wave equation using auxiliary differential equations (ade-pml).
Computer Modeling in Engineering and Sciences (CMES), 56(1):17.

Monteiller, V., Chevrot, S., Komatitsch, D., and Wang, Y. (2015).
Three-dimensional full waveform inversion of short-period teleseismic wavefields based upon the sem–dsm hybrid method.
Geophysical Journal International, 202(2):811–827.

Tromp, J., Tape, C., and Liu, Q. (2005).
Seismic tomography, adjoint methods, time reversal and banana-doughnut kernels.
Geophysical Journal International, 160(1):195–216.

Verschuur, D. and Berkhout, A. (1992).
Surface-related multiple elimination: practical aspects.
In *SEG Technical Program Expanded Abstracts 1992*, pages 1100–1103. Society of Exploration Geophysicists.

Virieux, J. (1986).
P-sv wave propagation in heterogeneous media: Velocity-stress finite-difference method.
Geophysics, 51(4):889–901.